Korean J. Chem. Eng., 40(4), 841-853 (2023)
DOI: 10.1007/s11814-022-1264-3

pISSN: 0256-1115
eISSN: 1975-7220

Design of novel hyper-branched dendritic boehmite/gallic acid alumoxane for methylene blue removal: Adsorption mechanism and reusability

Fatemeh Banisheykholeslami*, Morteza Hosseini*,†, Ghasem Najafpour Darzi*, and Mohammad Reza Shirzad Kebria*,**

*Department of Chemical Engineering, Babol Noshirvani University of Technology, Shariati Ave., Babol, Iran
**Smart Materials Group, Istituto Italiano di Tecnologia, via Morego 30, 16163 Genoa, Italy
(*Received 19 April 2022 • Revised 25 July 2022 • Accepted 17 August 2022*)

Abstract−A novel hyper-branched alumoxane with dendritic structure (Alu-Den) was prepared via a polycondensation reaction between hydroxyl groups of boehmite and carboxylic groups of gallic acid for use as an adsorbent for elimination of cationic Methylene blue from aqueous media. The successful formation of tree-like structure of Alu-Den was confirmed by several analyses, including FTIR, XRD, FE-SEM, BET, DLS and TGA. Adsorption variables, such as adsorbent dosage and pH, were optimized to acquire the maximum efficiency for dye removal. The results indicated that 0.02 g Alu-Den can totally eliminate 10 ml Methylene blue with concentration of 20 mg/l at 288 K and pH=10. In case of visionary investigation, the sorption process conformed to the pseudo-second-order kinetic model for all prepared concentrations. The Langmuir, Freundlich and Sips isotherms were evaluated to define the interaction between dye molecules and dendritic alumoxane structures. The results showed that the empirical data were in agreement with the Sips isotherm. Additionally, the spontaneous and exothermic quiddity of Methylene blue adsorption onto Alu-Den surface was divulged by thermodynamics assessments. Eventually, the Alu-Den was regenerated following four time adsorption-desorption cycles without significant loss in adsorption capacity. Hence, owing to its biocompatibility, simply accessible precursors, and high recyclability, the present novel adsorbent offered superior potential for the elimination of cationic dyes from aqueous phase.

Keywords: Adsorption, Boehmite, Alumoxane, Methylene Blue, Dendritic Structure

INTRODUCTION

Dye wastewater is known as one the most perilous threats to the environment and it can influence aquatic life intensely [1,2]. According to the analysis of the data presented by the Ecological and Toxicological Association of Dyes and synthetic organic pigments (ETAD) from 1974, more than 90% of some 4000 dyes assayed in an ETAD survey had LD_{50} (lethal dose 50%) quantities more than 2×10^3 mg/kg. The highest rates of toxicity were recognized amongst basic and diazo direct dyes [3]. Another survey concerning their toxicity towards fish, revealed that 98% of these dyes possess a CL_{50} (lethal concentration) greater than 1 mg/L, and 59% have a CL_{50} above 100 mg/L [4]. These values confirm the importance of studies on dye removal from aquatic medium.

Synthetic dyes are such resistant molecules against degradation arising from their aromatic structure. Methylene blue as a basic cationic dye which belongs to the thiazine family has plenty of applications in paper coloring [5], solar cells [6], wool or cotton dyeing, covering for paper stock [7], and as a impermanent hair color. Methylene blue is the prevalent dye in textile wastewater with many efforts made to eliminate it from water resources. Consequently, an efficient removal technique is required to avoid the potential problems originating from azo dye wastes to environment and human health. So far, different techniques have been introduced to eliminate dyes, including oxidation [8], nanofiltration [9,10], ozonation [11], photo-Fenton processes [12], photo-catalytic degradation [13], bio-treatment [14], clotting [15] and adsorption [16]. Among all these, adsorption is the most cost-effective and efficient process due to its safety, less energy consumption, simplicity and its sludge-free cleaning process [17].

Boehmite $[AlO(OH)]_n$ as oxide-hydroxides of aluminum with different water amounts and crystal sizes is widely used as adsorbent [18,19]. Besides, it is applied as a raw material for alumoxane production. Carboxylate-alumoxanes $[Al(O)_x(OH)_y(O2CR)_z]_n$ are synthesized through the reaction between boehmite with carboxylic acids (HO_2CR) with covalent bond. Carboxylate-alumoxane can be produced with an approximately infinite diversity of functional groups. The essential properties of alumoxane are the nature and scale of the joined organic groups. In fact, the alumoxane properties can be managed by selecting organic molecules. Alumoxane can be applied in synthesis of polymeric and bioabsorbable nanocomposites, membranes, coating materials and catalyst portions [20]. Alumoxane is introduced as a potential candidate for adsorption of contaminants from aqueous media due to its high specific surface area and appropriate structural properties which speed up the rate of mass transfer [18].

This work focuses on synthesis of a novel hyper-branched carboxylate-alumoxane with dendritic structure using boehmite and gallic acid as raw materials and its application in elimination of cationic dye (Methylene blue) from aqueous media. Gallic acid is a

†To whom correspondence should be addressed.
E-mail: m.hosseini@nit.ac.ir

Table 1. The specifications of the used dye

Dye	Molar mass (g/mol)	λ_{max} (nm)	Chemical formula	Chemical structure
Methylene blue	319.85	663	$C_{16}H_{18}ClN_3S$	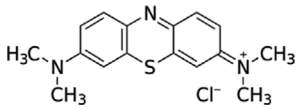

green, low-priced and available intrinsic polyphenol, which can be easily mined from plant tissue, bark, wood, fruit, tea and gallnuts [21]. Gallic acid also represents reliable advantages such as anti-carcinogenic, anti-mutagenic and anti-oxidant properties, low cost and ecofriendly nature. The impact of multiple parameters such as adsorbent dosage, solution pH, contact time and temperature on the maximum adsorption capacity was studied. With the aim of specifying the adsorption capability of the produced adsorbents, the adsorption isotherms, kinetics, thermodynamics as well as adsorbent reusability were also assessed.

MATERIALS AND METHODS

1. Materials

Aluminum nitrate nonahydrate ($Al(NO_3)_3{\cdot}9H_2O$, 98%), sodium hydroxide and gallic acid were provided by Merck (Germany) and utilized as precursors for synthesis of boehmite and alumoxane. Also, methylene blue was obtained from Merck. Table 1 gives the detailed information of purchased methylene blue. Acid and base content of the solutions were controlled by 0.1 M NaOH and HCl. All chemicals were consumed without further treatment.

2. Procurement of Boehmite Particles

The boehmite particles were produced via following protocols: i) certain amount of sodium hydroxide (6.49 g) and aluminum nitrate nonahydrate (20 g) were dissolved in specified amount of deionized water (50 ml, 30 ml), respectively; ii) sodium hydroxide solution was poured into the aluminum nitrate nonahydrate solution dropwise using intense stirring within 17 min. Then, the acquired slurry mixture was exposed to ultrasonic waves for 3 h at 25 °C. The obtained precipitate was heated in an oven for 4 h at 220 °C. Finally, the precipitate was rinsed and then purified using centrifugation method. The precipitate was dried at 70 °C before experiments.

3. Preparation of Carboxylate-alumoxane

Initially, 1.5 g of boehmite particles and 4.7 g gallic acid were totally mixed in 80 ml deionized water to attain a homogeneous mixture. The mixture was sonicated for 10 min in an ultrasonic bath at 25 °C. The acquired suspension was then heated under reflux condition at its boiling point for 24 h. Then, the suspension was put aside for cooling at room temperature. Before usage, the prepared powder was purified and dried in an oven at 70 °C for 24 h. A schematic of possible network of synthesized Alu-Den structures is shown in Fig. 1.

4. Characterization

The existence of diverse functional groups of boehmite particles and Alu-Den adsorbent was investigated by employing Fourier transform infrared spectroscopy (FTIR, BFRL WQF-510A) at the range of 400-4,000 cm^{-1}. X-ray diffraction (XRD) pattern of

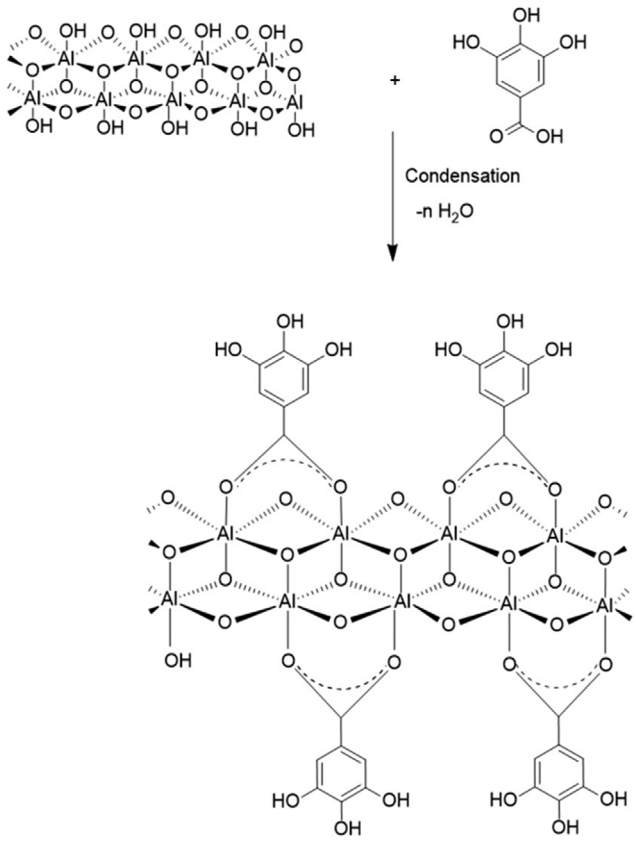

Fig. 1. Possible network of Alu-Den structure.

samples was achieved employing Panalytical X'Pert Pro (England). The thermal features of boehmite particles and Alu-Den were assessed via thermal gravimetric Analysis (TGA, TG 209F3 NETZSCH, Germany) under N_2 atmosphere (temperature range=25-800 °C, increasing rate=20 °C/min). The effective surface area was obtained using Brunauer-Emmett-Teller (BET) theory (Belsorp mini II, Japan). The structural and morphological aspects of the adsorbents were studied using field emission scanning electron microscopy (FE-SEM, MIRA3TESCAN, XUM). Before imaging, the particles were surface coated by gold under a spurring voltage of 20 k. The structure of the Alu-Den particles was also observed using a high magnification biological microscope (Nikon,YS100). Furthermore, the size distribution of the prepared adsorbents was analyzed through dynamic light scattering (DLS, SZ-100z, Horiba Jobin Jyovin) at room temperature.

5. Adsorption Assessment

Adsorption capacity of the prepared particles was investigated upon existence of Methylene blue using a noncontinuous adsorption system. A stock solution including 500 mg/l of Methylene blue

was provided using deionized water as solvent. Then, to choose reference concentration, different concentrations ranging from 5 to 30 ppm were prepared using various dilution factors. After a precise study, a solution containing 20 mg/l of MB was selected for the rest of experiments. To begin dye removal evaluations, initially, 10 ml of the mixture possessing given amount of adsorbents and dye solution was infused in 100 ml Erlenmeyer flasks. Then, the containers were shaken employing a shaker incubator at 200 rpm for a certain duration. The obtained suspension was centrifuged to collect used adsorbent. The concentration of residual Methylene blue particles in aqueous media was admeasured via a UV-Vis spectrophotometer (UV2100, UNICO). Eventually, adsorption capacity along with removal efficiency was attained by introduced expressions:

$$q_e = \frac{(C_0 - C_e)V}{m} \quad (1)$$

$$R = \frac{(C_0 - C_e)}{C_0} \times 100 \quad (2)$$

where q_e represents the equilibrium adsorption capacity (mg/g), R is the removal efficiency, C_0, C_e, m, and V introduce the initial dye concentration (mg/l), the dye concentration (mg/l) at equilibrium state, the amount of adsorbent (g) and the volumetric content of the dye solution (L), respectively.

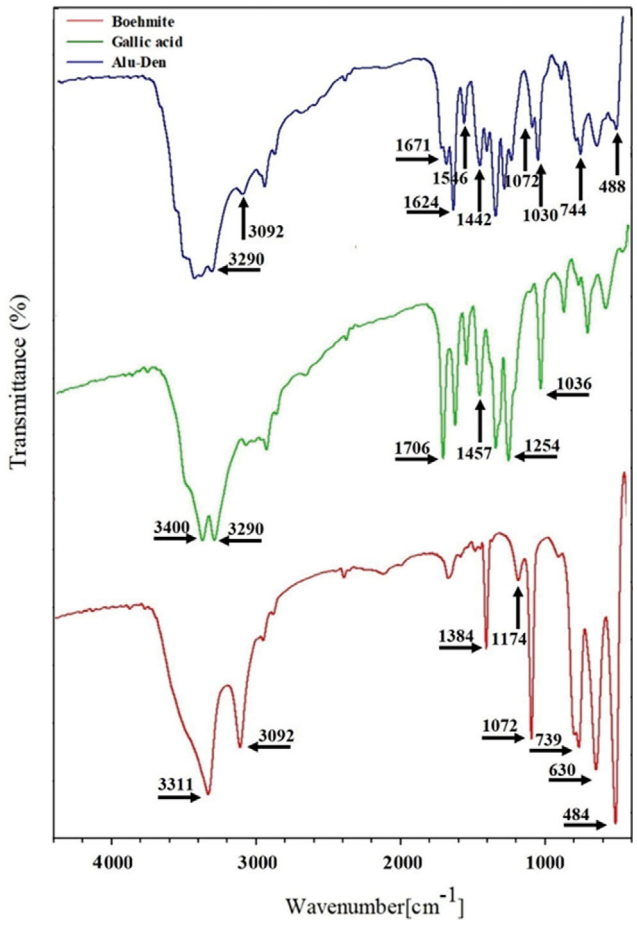

Fig. 2. FTIR spectra of boehmite, gallic acid and Alu-Den.

6. Regeneration Experiment

Renewability of Alu-Den adsorbent was assessed via consecutive adsorption-desorption cycles. With the aim of performing regeneration procedure, the used particles (0.02 g of Alu-Den) were poured into 10 ml of 2 M HCl solution. Thereupon, the mixture was shaken at 298 K for 3 h. The renewed adsorbents were purified, washed and dried. Afterwards, the dried adsorbents were taken into action for the subsequent adsorption cycle. The procedure was replicated four times to evaluate the reusability of the produced adsorbent.

RESULTS AND DISCUSSION

1. Characterization

FTIR spectra of boehmite particles, gallic acid and Alu-Den reis provided in Fig. 2. The FTIR spectra of boehmite particles are in agreement with the previous published data [18,22,23]. Couple of intensive bonding at 3,092 and 3,311 cm^{-1} correlate with the stretching hydroxyl related to Al-OH band. The absorption peaks at 732, 607 and 484 cm^{-1} are ascribed to the vibration mode of Al-O binding. Also, the observed absorption peak at 1,384 cm^{-1} is due to the stretching vibration of the nitrate ion impurity. The decline in peak intensity at 1,706 cm^{-1} for the relevant spectra of Alu-Den compared to the gallic acid spectra, confirms the creation of C-O-Al binding. Moreover, the reduction in peak strength at 1,615 cm^{-1} could be assigned to the conversion of the phenolic C-O in gallic acid to C-O-Al in Alu-Den as a consequence of reaction between gallic acid and boehmite.

XRD evaluation was carried out to assess crystalline structure of synthetic powder. Fig. 3 displays the XRD patterns of boehmite and Alu-Den particles. All characteristic peaks of boehmite particles were well-matched with standard peaks of AlOOH [1,22]. The pres-

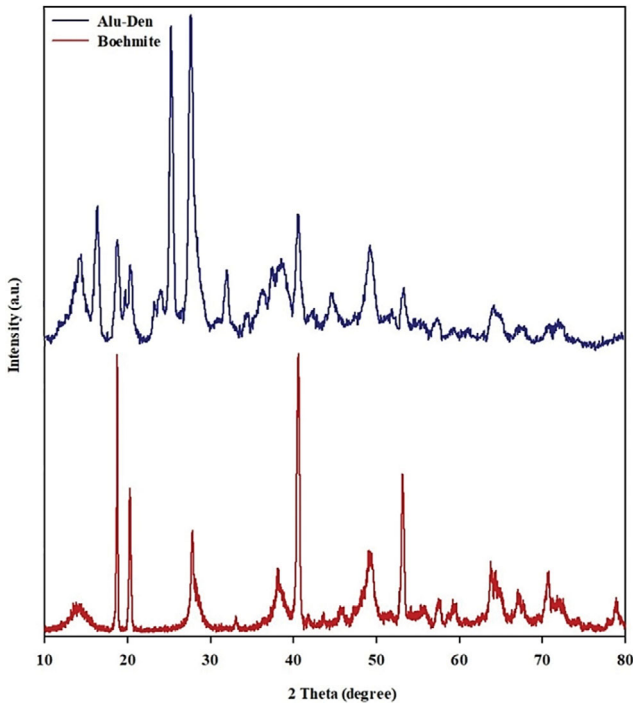

Fig. 3. XRD spectra of synthesized samples.

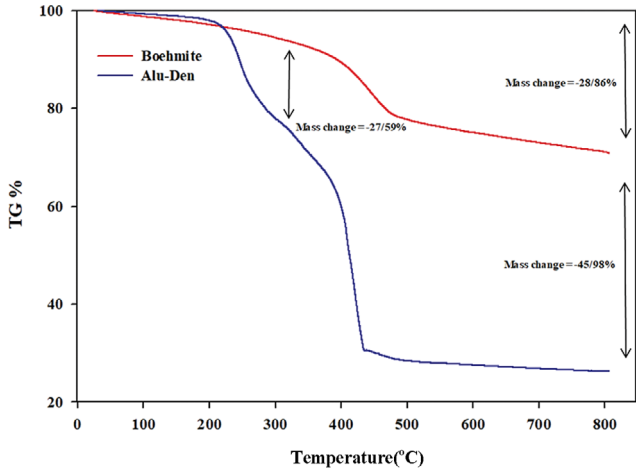

Fig. 4. TGA analysis of synthesized samples.

ence of sharp intensive peaks in the Alu-Den specimen confirms high crystallinity of the prepared alumoxane. As a matter of fact, the crystalline structure of the Alu-Den originated from the existence of boehmite particles. All the peaks detected in the XRD pattern of boehmite particles are also present in the XRD pattern of the Alu-Den sample. These peaks are in a similar angular position, indicating that the boehmite particles are well-embedded in the Alu-Den structure.

The TGA analysis results for Alu-Den and boehmite particles are presented in Fig. 4. The TGA analysis is broadly applied to admeasure weight variations and assess the thermal stability of a substance [24]. Based on the diagram of boehmite particles, a weight loss of 28.86% can be observed up to 500 °C that is attributed to the decomposition of hydroxyl bindings. The diagram also depicts that the residual weight of the boehmite sample at 800 °C is 71.1%, which confirms the high thermal stability of boehmite. Instead, the thermal stability of boehmite changed after reaction with gallic acid. Alu-Den particles showed two major decomposition stages. The primary decomposition stage happened at the temperature range of 200-350 °C (weight loss of 27.59%), which is ascribed to the loss of moisture and decomposition of hydroxyl bonds in the sample as well as internal dehydration. The next decomposition occurred in the temperature range of 350-800 °C (weight loss of 45.98%), which is attributed to the breakage of Carboxyl bonds and rings of Alu-Den. By comparing the degradation temperatures of the two samples, it can be found out that due to the linkage of gallic acid to the surface of boehmite particles, the weight loss in Alu-Den sample is 47% higher than that of boehmite particles, which

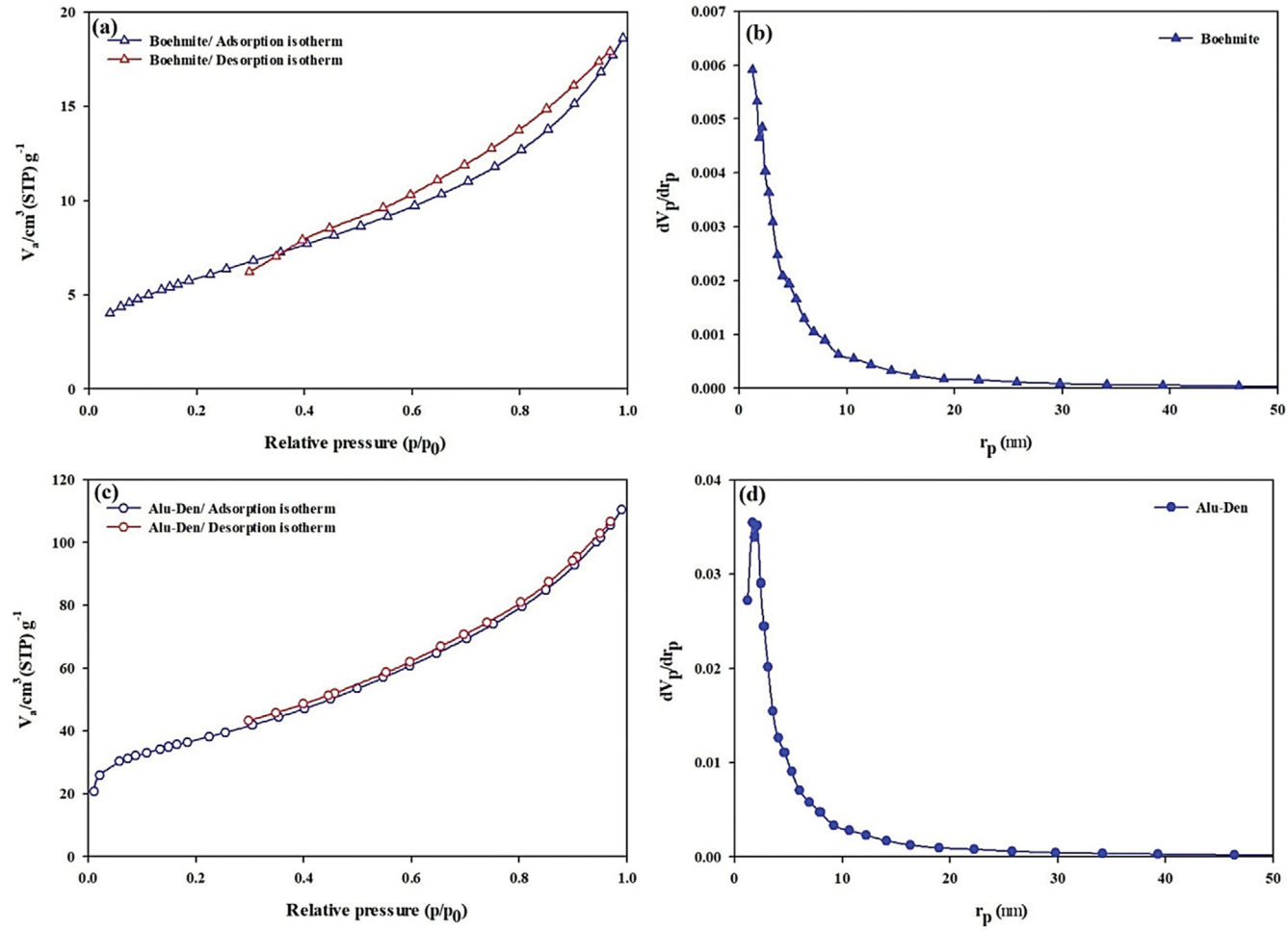

Fig. 5. N_2 adsorption-desorption isotherms (a) and (c) and BJH pore size distribution (b) and (d) of the boehmite and Alu-Den particles.

Table 2. The structural properties of boehmite and Alu-Den adsorbent

Adsorbent	S_{BET} (m^2/g)	Total pore volume (cm^3/g)	Mean pore diameter (nm)
Boehmite	21.474	0.02871	5.3478
Alu-Den	131.64	0.1708	5.1898

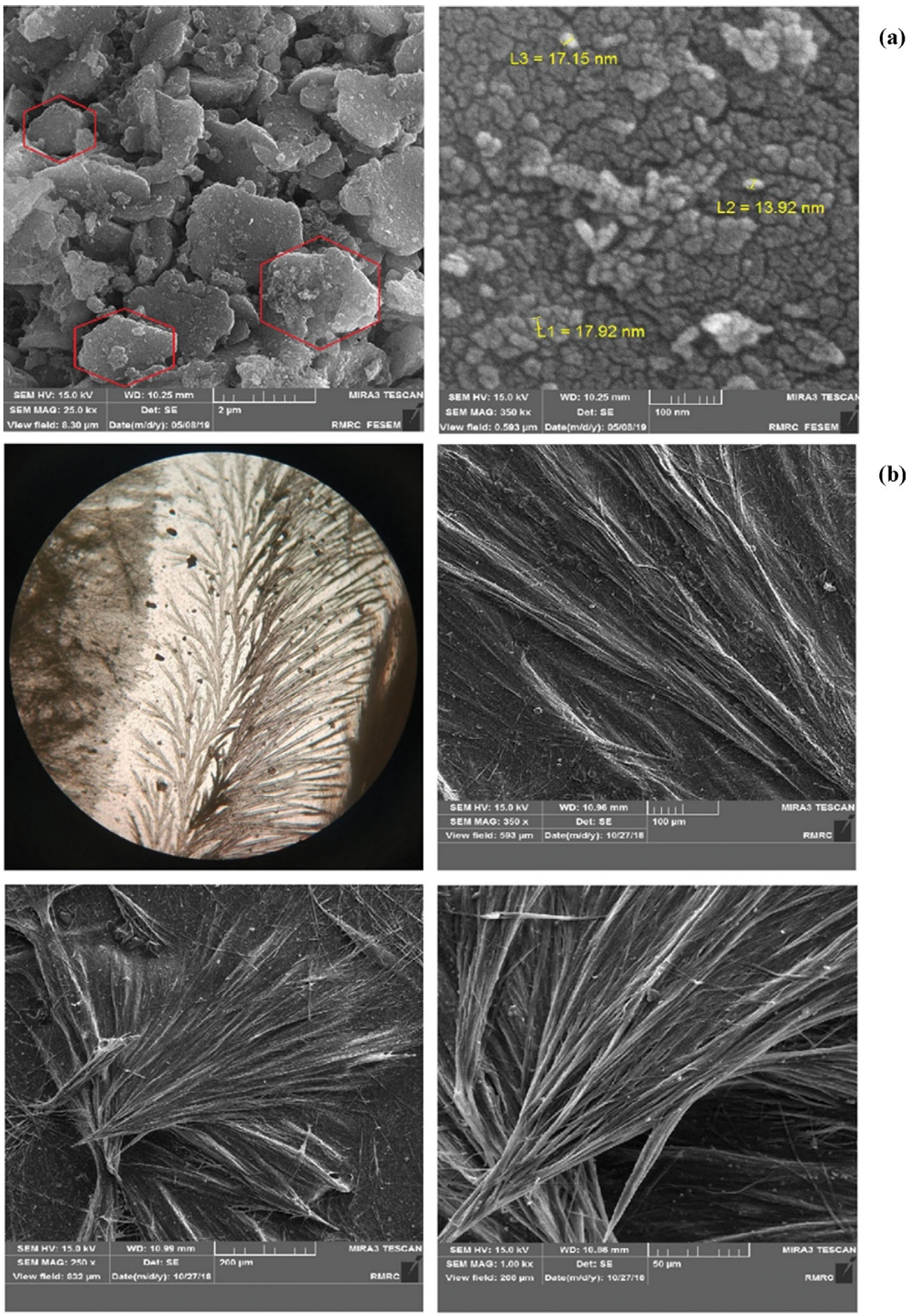

Fig. 6. FE-SEM images of the boehmite (a) and Alu-Den (b) particles in low and high magnifications.

is attributed to the degradation of carboxyl groups. From the TGA analysis of the synthesized adsorbent, it can be concluded that the materials can be used even at higher temperatures in water treatment.

The textural properties of boehmite and Alu-Den particles are shown in Fig. 5. N_2 adsorption-desorption isotherms were in agreement with the type IV adsorption isotherms of the IUPAC classification, indicating that both adsorbents were mesoporous [1]. Also Figs. 5(b) and (d) show pore size distribution diagram (BJH desorption diagram) of boehmite and Alu-Den, implying their mesoporosity with mean pore diameter of 5.3 and 5.1 nm, respectively. The BET specific surface area (S_{BET}) and specific cavity volume of Alu-Den were 131.64 m^2/g and 0.17 cm^3/g, respectively. Having a comparatively wide specific surface area, cavity volume, and high porosity gives multiple active sites to interact more capably in comparison with boehmite particles with BET specific surface area of 21.47 m^2/g and specific cavity volume of 0.028 cm^3/g. The values of S_{BET}, V_t as well as mean pore diameter of samples are listed in Table 2.

The FE-SEM images of the synthesized boehmite and Alu-Den samples with different magnifications as well as digital microscope image of Alu-Den are in Fig. 6. In Fig. 6(a), a single boehmite particle represents a polygonal, hexagonal or quasi-hexagonal structure. It also can be observed that in some areas the strong binding of hydrogen between several Al-OH groups causes agglomeration of boehmite particles. Fig. 6(b) also demonstrates the morphology of the Alu-Den structure in the filamentous shape originating from reaction between boehmite and gallic acid. Digital microscope image of Alu-Den confirms the tree-like structure and hyper-branched network of Alu-Den particles. Furthermore, FE-SEM images of the dendrimeric particles clearly show the dendritic growth of the branches. Additionally, the grooved fibrous structure of Alu-Den particles was confirmed by the FE-SEM images. Significant differences in the morphology of boehmite particles and synthesized alumoxane are mostly related to the various structural properties of the utilized precursors.

Fig. 7 displays particle size distributions of Alu-Den. From DLS diagrams, it can be concluded that Alu-Den has a mean particle size of 400 nm.

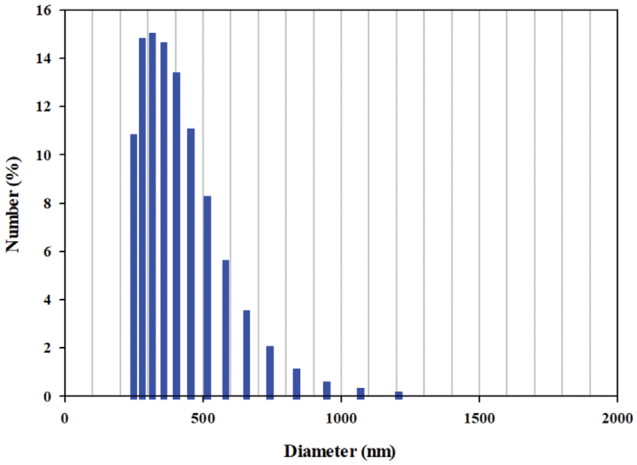

Fig. 7. DLS analysis of Alu-Den.

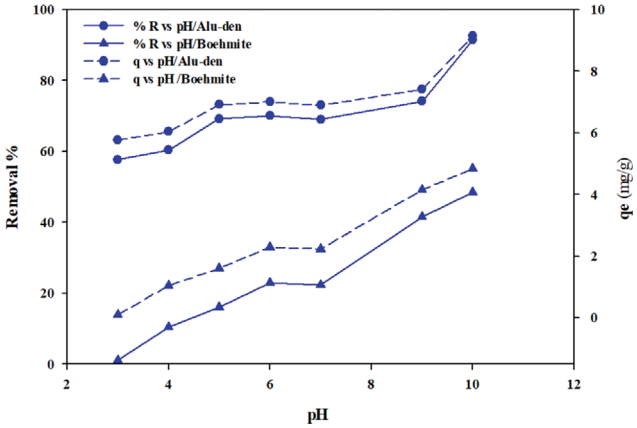

Fig. 8. Influence of pH on elimination and adsorption capacity of Methylene blue onto boehmite and Alu-Den particles (adsorbent dosage=0.02 g, T=298 K, and contact time=60 min).

2. Dye Removal Evaluation

2-1. Effect of pH

Effect of pH on the removal and adsorption capacity of Methylene blue onto the boehmite and Alu-Den is shown in Fig. 8. The pH value of the dye solution significantly influences the entire adsorption experiments and especially the sorption capacity. After several tests, it was concluded that the removal efficiency and sorption capacity improved upon increasing of pH values in the assessed

Table 3. Summary of the best pH for Methylene blue adsorption vs. adsorbent dosage variation

Adsorbent	pH	Adsorbent dosage	Removal (%)	Reference
Rice hulls	3-10	10 g/l	72-94%	[28]
Activated carbon obtained from Citrullus lanatus rind	2-10.94	0.001 g/ml	70-98%	[29]
$MgFe_2O_4$@SiO_2 NPs	3-11	0.042 g/15 ml	8-97%	[30]
Peach shell	2-12	0.4 g/100 ml	78-97.7%	[31]
Carbon Nanotube-based aerogels	2.5-12	0.25 g/25 ml	5-99%	[32]
Walnut shell	2-11	1.25 g/l	67.8-99.5%	[33]
Ficus carica bast	2-12	0.5 g/100 ml	12-89%	[34]
Polyamide-vermiculite	3-10	0.15 g/l	35-75%	[35]
Magnetic Zeolite/Chitosan/Alginate	3-11	0.025 g/l	19-36%	[36]
Alu-Den	3-10	0.02 g/10 ml	57-98%	This study

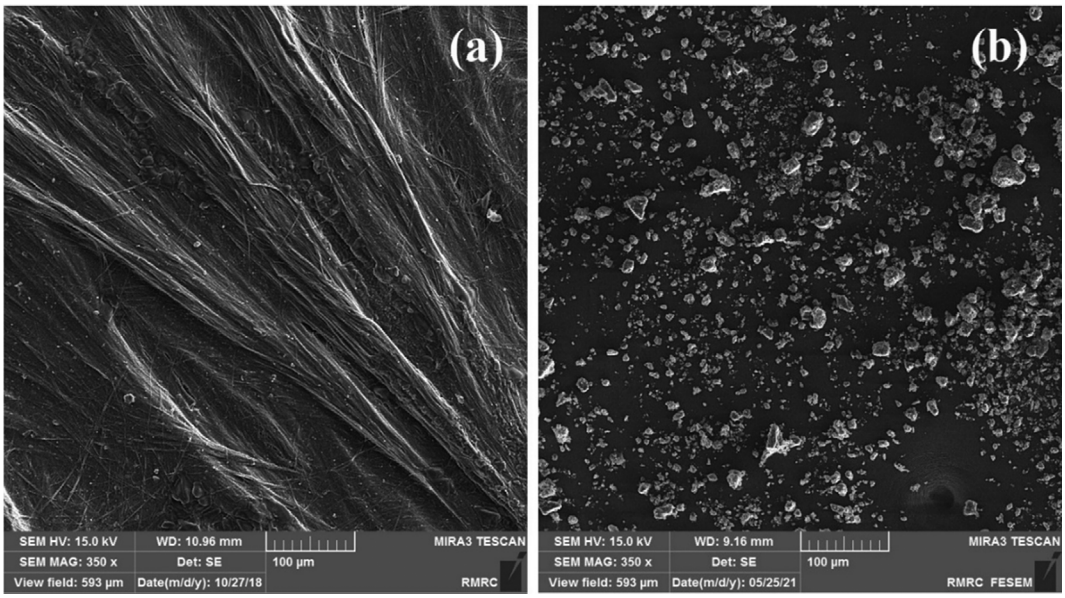

Fig. 9. FE-SEM images of Alu-Den in pH values ≤10 (a), pH values >10 (b).

domain. This result can be well described by the fact that at lower pH levels, contest between the excess number of protons (H^+) in the solution and the cationic MB for adsorption on the active sites of Alu-Den decreases the adsorption capacity, considering a certain number of active sites present on the sorbent. At higher pH values, with the decline in acidity of the media, cationic MB molecules are more able to be adsorbed onto the negatively charged sorbent containing many functional groups such as -COOH and -OH through electrostatic interactions. Therefore, moving from acidic to alkaline media enhances removal efficiency as well as adsorption capacity [25-27]. Table 3 summarizes the result of pH test for Methylene blue reported in other studies. In this study, the highest pH value (pH=10) was chosen to avoid the breakage of the Alu-Den structure. In addition to performance drop due to higher pH values, breakage of Alu-Den structure was confirmed by FE-SEM image (Fig. 9). In fact, by increasing of pH values, Alu-Den uniform filamentous structure converts to irregular lumpy structure as a result of degradation.

2-2. Effect of Adsorbent Dosage

To investigate the impact of Alu-Den amount on the sorption process, the removal percentage and sorption capacity of Methylene blue was evaluated using different contents of adsorbent (0.005-0.04 g). As represented in Fig. 10, the removal percentage of Methylene blue was specified to be enhanced with increasing the Alu-Den dosage and reached to maximum efficiency of 91.2% upon using 0.02 g of the adsorbent. Table 4 shows the obtained data for different adsorbent's dosage and their corresponding removal efficiency as well as adsorption capacity. As listed in Table 4, when adsorbent' dosage increased from 0.02 to 0.04 g, removal efficiency experienced a slight increase (from 91.2 to 93.04), while adsorption capacity declined from 9.12 to 4.65 mg/g. In fact, due to the presence of more active sites resulting from increase of sorbent dosage from 0.005 to 0.02 g, MB removal increased from 50.3 to 91.2%. On the other hand, with increasing of sorbent dosage from 0.02 to 0.04 g, adsorption capacity decreased, perceptibly. It might be attributed to the gap in the flux or the concentration variations between dye concentration in the bulk and the dye concentration

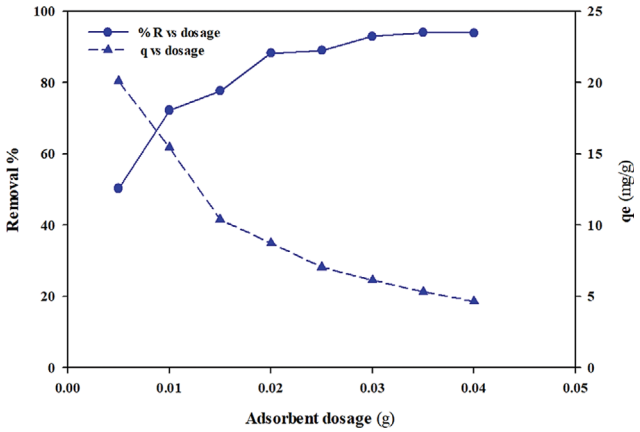

Fig. 10. Effect of adsorbent amount on the removal and sorption capacity of Methylene blue onto Alu-Den, (pH=10, T=298 K, and contact time=60 min).

Table 4. The results of MB removal using different sorbent's dosage

Adsorbent dosage (g)	Removal (%)	q (mg/g)
0.005	50.3	20.12
0.01	72.25	15.45
0.015	77.69	10.39
0.02	91.2	9.12
0.025	91.5	7.32
0.03	92.5	6.17
0.035	93.12	5.32
0.04	93.04	4.65

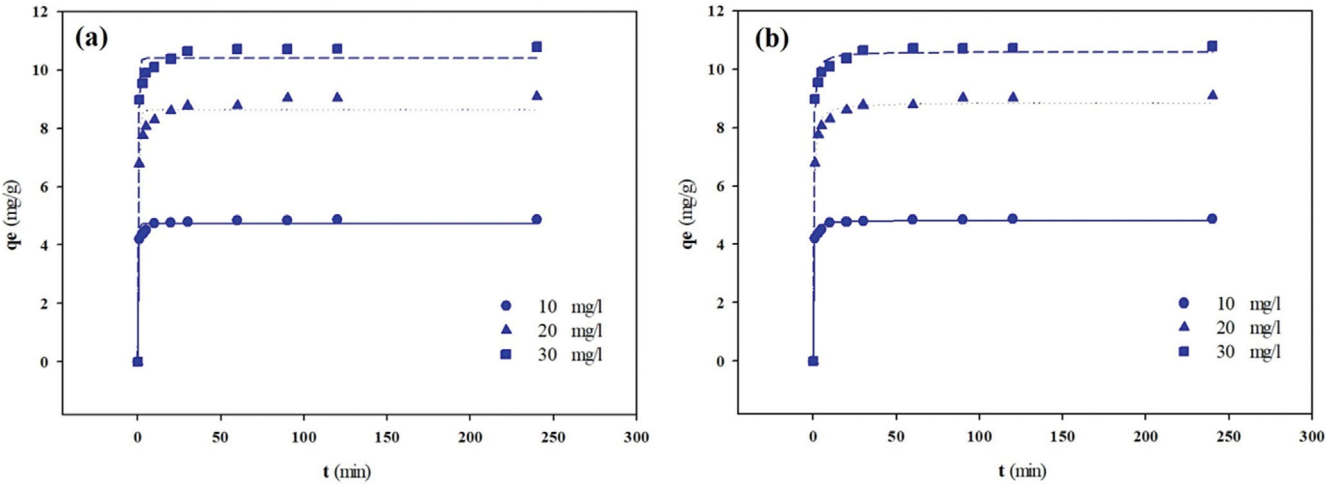

Fig. 11. Pseudo-first-order kinetic (a) and pseudo-second-order kinetic diagram (b) for the sorption of Methylene blue (Conditions: adsorbent dosage=0.02 g, contact time=240 min, pH=10, and T=298 K).

Table 5. Kinetic parameters for Methylene blue sorption onto Alu-Den

Kinetic model	Parameters	Initial Methyl blue concentration (mg/l)		
		10	20	30
Pseudo-first-order	K_1 (1/min)	2.1529	1.4813	1.9563
	$q_{e,cal}$ (mg/g)	4.7416	8.6233	10.3997
	R^2	0.9888	0.9764	0.9843
Pseudo-second-order	K_2 (g/mg·min)	1.1983	0.3241	0.4385
	$q_{e,cal}$ (mg/g)	4.8179	8.8637	10.6021
	R^2	0.9967	0.9948	0.9953

at the surface of the Alu-Den [37]. Also, this result can be well explained by the fact that when number of active sites increases by increasing of sorbent dosage and concentration gradient remains almost constant, adsorption capacity decreases [38,39]. Besides, by comparing the obtained data, it can be seen choosing 0.02 g as ideal dose makes the process economically efficient. Therefore, by taking these factors into account, 0.02 g of Alu-Den was chosen as ideal dose for the following dye removal experiments.

2-3. Adsorption Kinetics

The adsorption kinetics of positively charged Methylene blue onto the Alu-Den was studied using diverse dye concentrations (10, 20 and 30 mg/l). The outcomes are presented in Fig. 11 and Table 5. Based on the values in Fig. 11 and Table 5, although, the adsorption capacity of Alu-Den quickly increases during 10 min, the increasing rate drops until equilibrium is attained (after 60 min). Also, increasing the primary concentration of dye leads to the increase of adsorption capacity. Consequently, the dye removal efficiency relies on the initial dye content. The quantity of Methylene blue adsorbed at equilibrium increased from 4.87 to 11.79 mg/g as soon as the primary dye content increased from 10 to 30 mg/l. To explore the commanding protocol of the sorption, pseudo-first-order and pseudo-second-order kinetic models were employed using gained empirical data [40]:

$$\ln(q_e - q_t) = \ln q_e - K_1 t \quad (3)$$

$$\frac{t}{q_t} = \frac{1}{K_2 q_e^2} + \frac{t}{q_e} \quad (4)$$

where q_e and q_t (mg/g) introduce the sorption capacity within equilibrium and time t (min), in a given order. Also, K_1 (1/min) and K_2 (g/mg·min) represent the pseudo-first-order and pseudo-second-order rate constants, in a given order. Both pseudo-first-order and pseudo-second-order theories were used to analyze the sorption procedure. The obtained outcomes indicated that the pseudo-second-order pattern presented higher correlation factors offering better adjustment with the experimental data. Therefore, it is evident that chemisorption occurred on Alu-Den [41].

2-4. Adsorption Isotherm

The adsorption isotherms were studied to recognize the adsorption capacity of Alu-Den at different temperatures (288, 298, 308 and 318 K), an adsorbent amount of 0.02 g and a contact time of 60 min. Several preliminary concentrations of dye (5, 10, 20, 30 and 40 mg/l) were employed to evaluate the quantity of adsorbed Methylene blue. At given concentration, the quantity of adsorbed dyes raised with augmenting initial concentration until equilibrium state was achieved. In the present work, triple non-linear isotherms (Langmuir, Freundlich and Sips) were used to correlate with the empirical data. The empirical outcomes are in Fig. 12. Isotherm variables are listed in Table 6. The Langmuir isotherm (Fig. 12(a)) assumes that sorption happens upon homogeneous area forming

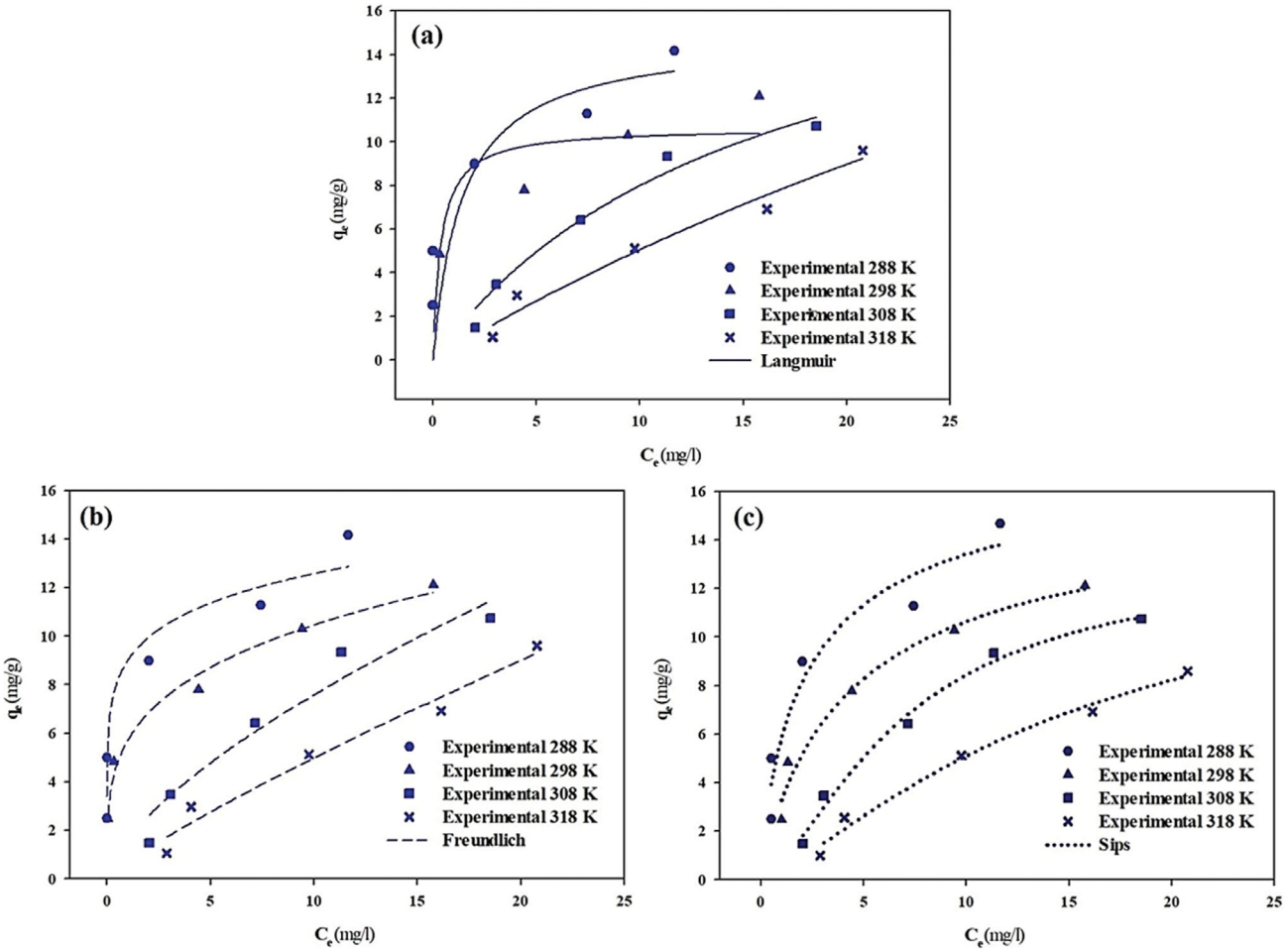

Fig. 12. Langmuir (a), Freundlich (b) and Sips (c) adsorption isotherms for Methylene blue removal onto the Alu-Den.

Table 6. Langmuir, Freundlich, and Sips model constants for the adsorption of Methylene blue on the Alu-Den

Isotherms	Parameters	Methylene blue			
		Temperature (K)			
		288 K	298 K	308 K	318 K
Langmuir	q_m (mg/g)	14.832	10.6418	20.584	39.297
	K_l (l/mg)	0.7049	2.6114	0.0636	0.0148
	R_L	0.0632	0.0179	0.4281	0.762
	R^2	0.6217	0.8647	0.9756	0.9675
Freundlich	K_f ((mg/g)(mg/l)$^{-1/n}$)	9.0012	5.7034	1.6325	0.6980
	N	6.887	3.7921	1.4985	1.1713
	R^2	0.9248	0.9857	0.9477	0.9692
Sips	q_m (mg/g)	14.4226	13.5158	13.0432	12.1723
	K_S ((mg/l)$^{-1/n_S}$)	0.4072	0.2134	0.054	0.0280
	n_S	2.083	1.1218	1.5143	1.3025
	R^2	0.9135	0.9981	0.9902	0.9831

a monolayer without chemical interaction. The non-linear format of the Langmuir isotherm is described in this way [42]:

$$q_e = \frac{q_m K_L C_e}{1 + K_L C_e} \quad (5)$$

where q_m, C_e, and K_L introduce the utmost sorption capacity (mg/g), the equilibrium concentration of dyes (mg/l) and the Langmuir constant pertinent to the energy of adsorption (l/mg), in a given order. Additionally, R_L, that is known as Langmuir sequestering factor, is computed using Eq. (6) [43]:

$$R_L = \frac{1}{1+K_L C_{0m}} \quad (6)$$

where, C_{0m} (mg/l) introduces the average initial concentration of dyes. The R_L values identify the kind of the adsorption method to be unfavorable (R_L>1), linear (R_L=1), favorable (0<R_L<1), or irreversible (R_L=0).

Freundlich isotherm (Fig. 12(b)) supposes that sorption occurs over a multilayer sorption on the heterogeneous area that can be described by the equation below [44]:

$$q_e = K_F C_e^{1/n} \quad (7)$$

where K_F represents a Freundlich isotherm constant ((mg/g)(mg/l)$^{-1/n}$) demonstrating the binding energy, and n introduces a constant attributed to adsorption strength. The value of 0<n<10 explains favorable adsorption [45].

The probable incongruity of sorption has also been investigated by Sips theory (Fig. 12(c)). The Sips theory is defined using Eq. (8) [46]:

$$q_e = \frac{q_m K_S C_e^{n_s}}{1+K_S C_e^{n_s}} \quad (8)$$

where K_S is the sorption constant of Sips ((mg/l)$^{-1/n_S}$) and n_S is the Sips incongruity coefficient.

Based on the achieved results, the q_m value for sorption of Methylene blue onto Alu-Den declined from 14.67 mg/g at 288 K to 8.6 mg/g at 318 K introducing the exothermic essence of the procedure. As can be seen from Table 6 and Fig. 12, conforming to the correlation coefficient values (R^2), the empirical data achieved from adsorption tests were well-suited with Sips theory. The adsorption mechanism of Methylene blue is multilayer and it takes place on inharmonious sites with different sorption energy. Following the Sips theory, the utmost adsorption capacity of Alu-Den was 14.42 mg/g (real sorption capacity=15.1 mg/g). Assuming Langmuir theory, the magnitude of R_L varies between 0<R_L<1, which specifies suitable adsorption of dye on Alu-Den at whole examined temperatures. Ultimately, all the magnitudes of n in Freundlich model were larger than 1, indicating a suitable adsorption process.

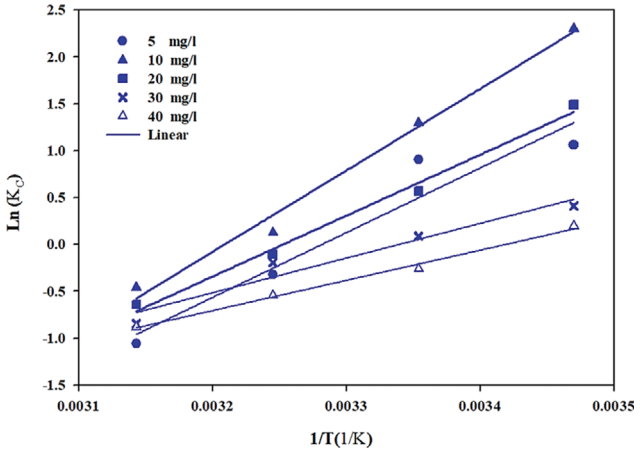

Fig. 13. Diagram of lnK$_c$ vs. 1/T for adsorption of Methylene blue on the Alu-Den.

2-5. Thermodynamics Study

The thermodynamics studies give encyclopedic view into the impact of temperature changes on sorption procedure. Thermodynamics variables such as enthalpy (ΔH^0), entropy (ΔS^0), and Gibbs

Table 7. Computed thermodynamics variables for adsorption of Methylene blue on Alu-Den

C_0 (mg/l)	Temperature (K)	R^2	ΔG (kJ/mol)	ΔS (J/mol)	ΔH (kJ/mol)
5	288	0.9232	−5.1537	−188.6912	−59.4968
	298		−3.266		
	308		−1.3799		
	318		0.501		
10	288	0.9888	−6.4780	−232.1069	−73.3248
	298		−4.1569		
	308		−1.8358		
	318		0.485		
20	288	0.9913	−4.4176	−175.9300	−55.0855
	298		−2.6583		
	308		−0.8990		
	318		0.860		
30	288	0.9473	−4.1764	−102.7311	−33.763
	298		−3.1491		
	308		−2.1218		
	318		−1.0945		
40	288	0.9934	−2.4090	−91.6676	−28.8102
	298		−1.4932		
	308		−0.5735		
	318		0.3400		

free energy (ΔG^0) were calculated to study the nature and spontaneity of the sorption process of Methylene blue on Alu-Den. The pertaining mathematical relations are provided as follows [47,48]:

$$K_C = \frac{C_s}{C_e} \quad (9)$$

$$\Delta G^0 = -RT\ln K_c = \Delta H - T\Delta S \quad (10)$$

$$\ln K_C = \frac{\Delta S^0}{R} - \frac{\Delta H^0}{RT} \quad (11)$$

where K_c introduces a constant defined as proportion of value of adsorbed dye on the surface of adsorbent (C_s (mg/l)) to the equilibrium dye concentration (C_e (mg/l)), T is the temperature (K) and R is defined as the ideal gas constant (8.314 J/mol·K). The values of ΔH^0 and ΔS^0 were extracted from the gradient and intercept of $\ln K_c$ vs 1/T plot, (van't Hoff plot, Fig. 13), respectively. The acquired data are summed up in Table 7.

As presented in Table 7, the negative magnitude of ΔH^0 shows the exothermic nature of adsorption of Methylene blue onto Alu-Den, which accords well with the values obtained from the adsorption models. Commonly, if the heat of sorption changes among 5-40 kJ/mol, the operation would be physisorption, while greater energies (60-240 kJ/mol) introduce chemisorption [49]. It can be seen that simultaneous physisorption and chemisorption happen for Methylene blue during the adsorption process. The negative magnitude of Gibbs free energy (ΔG^0) points out the probability and spontaneity of dye adsorption [50]. The negative magnitude of ΔS^0 describes a reduced randomness at the liquid-solid interface within the sorption [51,52].

2-6. Regeneration Studies

Ease of regeneration is an important factor in the adsorption process. Usually, thermal procedures or acid-base reactions are employed to desorb solutes [53]. In the present work, HCl 2 M was chosen as the carrier liquid for desorption. Fig. 14 displays the performance of revived adsorbents during elimination of Methylene blue. The outcomes demonstrate that the removal efficiency of Alu-Den declined as the number of cycles increased. This happens owing to the seizure of active sites and lack of adequate reactive functional groups on the surface of Alu-Den particles. However, after the fourth cycle, the removal efficiency is still higher than 50%, indicating high efficiency of Alu-Den particle for the filtration of effluents comprising organic dyes.

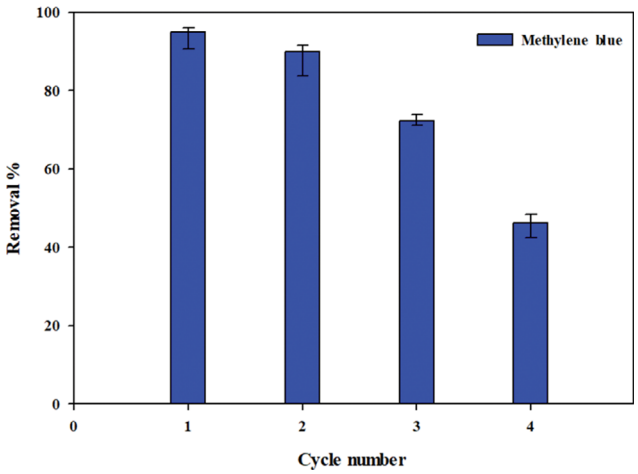

Fig. 14. Regeneration performance of Alu-Den adsorbent toward Methylene blue dye in four successive cycles of adsorption-desorption.

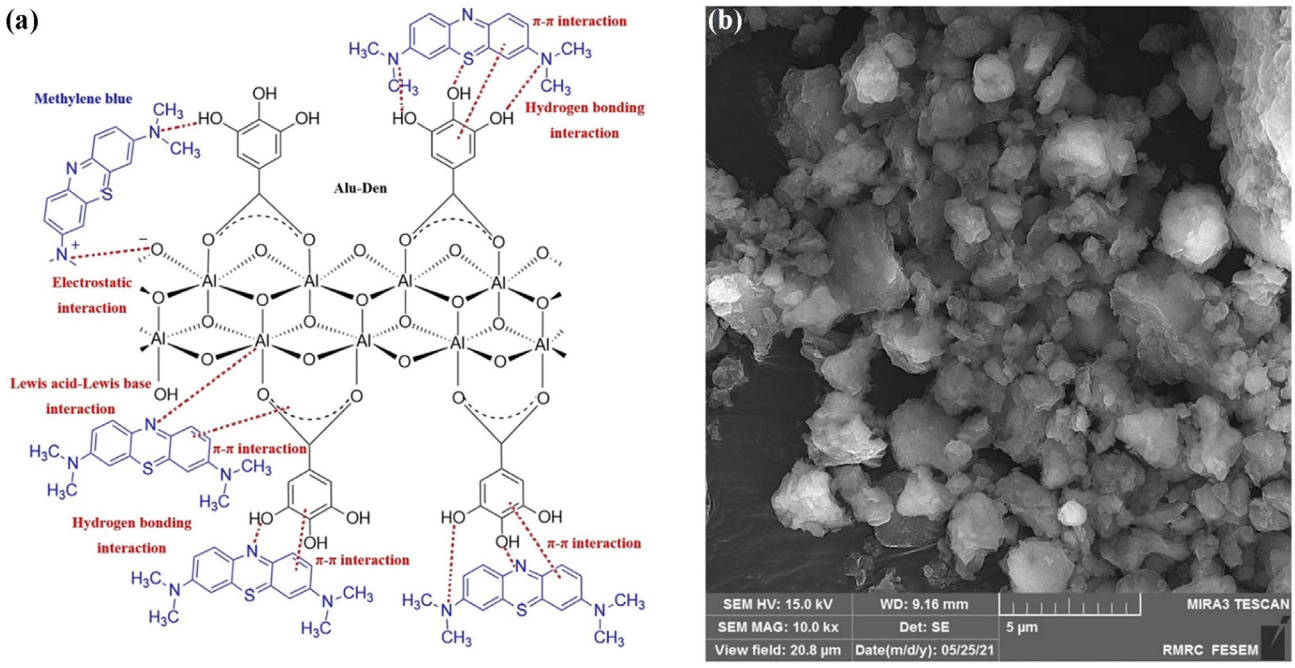

Fig. 15. Possible Methylene blue adsorption mechanism onto Alu-Den (a) and FE-SEM image of Alu-Den adsorbent after Methylene blue adsorption (b).

2-7. Adsorption Mechanism

The adsorption of Methylene blue onto the surface of alumoxane particles can be described by four possible mechanisms; see Fig. 15(a). The first corresponds to the hydrogen binding formed between alumoxane particles and dye molecules. Thus, Methylene blue molecules show a propensity to interact with the hydrogen atoms available in the -OH group of Alu-Den particles due to the presence of nitrogen (N) and sulfur (S) atoms in their structure. The subsequent mechanism could be attributed to the interactions among heteroatoms (N, S) and Al atoms available in the alumoxane nucleus [54]. While Al atoms operate as Lewis acid, N and S atoms are representatives of Lewis base family. The result clearly proves that the sorption capacity of Alu-Den for Methylene blue was higher than that of boehmite particles, which corroborates that the functionalized boehmite with benzene ring improved the π-π conjugation between the Alu-Den and the aromatic Methylene blue. The π-π interaction can occasionally make strong interplays between adsorbents and adsorbates, leading to improved adsorption capacity. Also, Methylene blue is a cationic dye which shows a high tendency to stick easily onto the negatively charged surface of Alu-Den via electrostatic forces [29,38]. Also, Fig. 15(b) displays the FE-SEM image of Alu-Den particles after adsorption of Methylene blue molecules. As displayed in Fig. 15(b), most of the pores of the Alu-Den particles have been blocked as a result of adsorption of Methylene blue.

CONCLUSION

A novel hyper-branched dendritic alumoxane (Alu-Den) was produced through a polycondensation reaction among hydroxyl groups of boehmite and carboxylic groups of gallic acid. It was observed that boehmite adsorption capability was improved after surface modification by gallic acid. Effect of pH and different Alu-Den amount was also investigated. In alkaline media, adsorbent showed better performance than acidic one causing to choose pH=10 as an optimum pH for adsorption of Methylene blue onto Alu-Den adsorbent. Among the adsorption models, the Langmuir presented the best accordance with empirical data. In case of kinetics, the adsorption process followed a pseudo-second order theory. The thermodynamic studies suggested that Methylene blue adsorption onto Alu-Den was chemisorption, spontaneous at low temperature and exothermic. Thus, Alu-Den is a promising adsorbent for elimination of Methylene blue from an aqueous media, and it can be considered as a capable and low-cost alternative to other available adsorbents. Alu-Den can also be applied as a suitable adsorbent for the elimination of cationic dyes from effluent.

ACKNOWLEDGEMENT

The authors would like to appreciate Babol Noshirvani University of Technology for providing financial support by awarding a research grant (Grant No.: BNUT/955150003/2019).

COMPETING INTERESTS

The authors declare that they have no known competing financial interests or personal relationships that could have appeared to influence the work reported in this paper.

AUTHOR CONTRIBUTIONS

Conceptualization, writing, and original draft preparation were performed by Fatemeh Banisheykholeslami. Investigation was carried out by Fatemeh Banisheykholeslami, and Mohammad Reza Shirzad Kebria. Methodology, and project administration were done by Morteza Hosseini. Also, supervision was performed by Morteza Hosseini, and Ghasem Najafpour Darzi. Finally, review and editing were accomplished by Morteza Hosseini, Ghasem Najafpour Darzi, and Mohammad Reza Shirzad Kebria. All authors read and approved the final manuscript.

ETHICAL APPROVAL

The authors mentioned in the manuscript have agreed for authorship, read and approved the manuscript, and given consent for submission and subsequent publication of the manuscript.

CONSENT TO PARTICIPATE

Not applicable.

CONSENT TO PUBLISH

Not applicable.

AVAILABILITY OF DATA AND MATERIALS

The authors declare that data supporting the findings of this study are available within the article.

REFERENCES

1. S. Ghabaee, J. Behin, M. Ansari and L. Rajabi, *Adv. Powder Technol.*, **31**, 2061 (2020).
2. L. Laasri, M. Khalid Elamrani and O. Cherkaoui, *Environ. Sci. Pollut. Res.-Int.*, **14**, 237 (2007).
3. T. Robinson, G. McMullan, R. Marchant and P. Nigam, *Bioresour. Technol.*, **77**, 247 (2001).
4. M. Berradi, R. Hsissou, M. Khudhair, M. Assouag, O. Cherkaoui, A. El Bachiri and A. El Harfi, *Heliyon*, **5**, e02711 (2019).
5. L. Gan, S. Shang, E. Hu, C. W. M. Yuen and S.-x. Jiang, *Appl. Surf. Sci.*, **357**, 866 (2015).
6. M. Muzakkar, D. Wibowo and M. Nurdin, *IOP Conference Series: Mater. Sci. Eng.*, **267**, 012035 (2017).
7. V. Katheresan, J. Kansedo and S. Y. Lau, *J. Environ. Chem. Eng.*, **6**, 4676 (2018).
8. T.-H. Kim, C. Park, J. Yang and S. Kim, *J. Hazard. Mater.*, **112**, 95 (2004).
9. M. R. S. Kebria, M. Jahanshahi and A. Rahimpour, *Desalination*, **367**, 255 (2015).
10. M. Shirzad Kebria, *Int. J. Eng.*, **27**, 1173 (2014).
11. M. Muthukumar and N. Selvakumar, *Dyes Pigm.*, **62**, 221 (2004).

12. A. Alayli, H. Nadaroglu and E. Turgut, *Appl. Water Sci.*, **11**, 1 (2021).
13. Y. Dong, Z. Han, C. Liu and F. Du, *Sci. Total Environ.*, **408**, 2245 (2010).
14. S. Mishra, L. Cheng and A. Maiti, *J. Environ. Chem. Eng.*, **9**, 104901 (2021).
15. B. Shi, G. Li, D. Wang, C. Feng and H. Tang, *J. Hazard. Mater.*, **143**, 567 (2007).
16. B. Mu and A. Wang, *J. Environ. Chem. Eng.*, **4**, 1274 (2016).
17. M. F. R. Pereira, S. F. Soares, J. J. Órfão and J. L. Figueiredo, *Carbon*, **41**, 811 (2003).
18. A. A. Derakhshan and L. Rajabi, *Powder Technol.*, **226**, 117 (2012).
19. A. P. Panda, U. Jha and S. Swain, *J. Water Process Eng.*, **37**, 101506 (2020).
20. S. J. Obrey and A. R. Barron, *J. Chem. Soc., Dalton Trans.*, 2456 (2001).
21. E. Haslam and Y. Cai, *Nat. Prod. Rep.*, **11**, 41 (1994).
22. M. R. S. Kebria, A. Rahimpour, S. K. Salestan, S. F. Seyedpour, A. Jafari, F. Banisheykholeslami and N. T. H. Kiadeh, *Desalination*, **479**, 114307 (2020).
23. L. Rajabi and A. Derakhshan, *Sci. Adv. Mater.*, **2**, 163 (2010).
24. F. Banisheykholeslami, A. A. Ghoreyshi, M. Mohammadi and K. Pirzadeh, *CLEAN–Soil, Air, Water*, **43**, 1084 (2015).
25. M. Dubey, S. Wadhwa and R. Kumar, *Mater. Today: Proceedings*, **28**, 70 (2020).
26. M. A. Farghali, M. M. Abo-Aly and T. A. Salaheldin, *Inorg. Chem. Commun.*, **126**, 108487 (2021).
27. P. Sirajudheen, P. Karthikeyan, S. Vigneshwaran and S. Meenakshi, *Int. J. Biol. Macromol.*, **175**, 361 (2021).
28. A. El-Maghraby and H. El Deeb, *Global NEST J.*, **13**, 90 (2011).
29. O. Üner, Ü. Geçgel and Y. Bayrak, *Water, Air, Soil Pollut.*, **227**, 1 (2016).
30. S. Hoijang, S. Wangkarn, P. Ieamviteevanich, S. Pinitsoontorn, S. Ananta, T. R. Lee and L. Srisombat, *Colloids Surf. A: Physicochem. Eng. Aspects*, **606**, 125483 (2020).
31. S. Marković, A. Stanković, Z. Lopičić, S. Lazarević, M. Stojanović and D. Uskoković, *J. Environ. Chem. Eng.*, **3**, 716 (2015).
32. N. Tabrizi and M. Yavari, *Chem. Eng. Res. Des.*, **94**, 516 (2015).
33. R. Tang, C. Dai, C. Li, W. Liu, S. Gao and C. Wang, *J. Chem.*, **2017** (2017).
34. D. Pathania, S. Sharma and P. Singh, *Arabian J. Chem.*, **10**, S1445 (2017).
35. A. A. Basaleh, M. H. Al-Malack and T. A. Saleh, *J. Environ. Chem. Eng.*, **7**, 103107 (2019).
36. J. Kazemi and V. Javanbakht, *Int. J. Biol. Macromol.*, **154**, 1426 (2020).
37. P. Wang, Q. Ma, D. Hu and L. Wang, *React. Funct. Polym.*, **91**, 43 (2015).
38. S. Bagherpour, M. Riazi, M. Riazi, F. B. Cortés and S. H. Mousavi, *ACS Omega*, **5**, 16149 (2020).
39. Y.-M. Hao, C. Man and Z.-B. Hu, *J. Hazard. Mater.*, **184**, 392 (2010).
40. S. U. Jan, A. Ahmad, A. A. Khan, S. Melhi, I. Ahmad, G. Sun, C.-M. Chen and R. Ahmad, *Environ. Sci. Pollut. Res.*, **28**, 10234 (2021).
41. F. Banisheykholeslami, M. Hosseini and G. N. Darzi, *Int. J. Biol. Macromol.*, **177**, 306 (2021).
42. J. Singh and A. Dhaliwal, *J. Polym. Environ.*, **29**, 71 (2021).
43. B. Kannamba, K. L. Reddy and B. AppaRao, *J. Hazard. Mater.*, **175**, 939 (2010).
44. H. Freundlich, *J. Phys. Chem.*, **57**, 1100 (1906).
45. R. R. Bhatt and B. A. Shah, *Arabian J. Chem.*, **8**, 414 (2015).
46. D. Balarak, J. Jaafari, G. Hassani, Y. Mahdavi, I. Tyagi, S. Agarwal and V. K. Gupta, *Colloids Interface Sci. Commun.*, **7**, 16 (2015).
47. H. Ge, T. Hua and X. Chen, *J. Hazard. Mater.*, **308**, 225 (2016).
48. M. Saeed, M. Munir, M. Nafees, S. S. A. Shah, H. Ullah and A. Waseem, *Micropor. Mesopor. Mater.*, **291**, 109697 (2020).
49. A. Zahir, Z. Aslam, M. S. Kamal, W. Ahmad, A. Abbas and R. A. Shawabkeh, *J. Mol. Liq.*, **244**, 211 (2017).
50. M. Rahman and K. V. Sathasivam, *BioMed Res. Int.*, **2015**, 126298 (2015).
51. R. Lotfi, B. Hayati, S. Rahimi, A. A. Shekarchi, N. M. Mahmoodi and A. Bagheri, *Microchem. J.*, **146**, 1150 (2019).
52. P. Rai, R. K. Gautam, S. Banerjee, V. Rawat and M. Chattopadhyaya, *J. Environ. Chem. Eng.*, **3**, 2281 (2015).
53. Y. Zhou, J. Lu, Y. Zhou and Y. Liu, *Environ. Pollut.*, **252**, 352 (2019).
54. N. N. Nassar, A. Hassan and P. Pereira-Almao, *J. Colloid Interface Sci.*, **360**, 233 (2011).